MTTM

Megha-Tropiques Technical Memorandum

Composite of Convective Systems: a Megha-Tropiques product

Algorithm Theoretical Basis Document

Thomas Fiolleau, Rémy Roca, Jérémie Aublanc, Olivier Chomette, Patrick Raberanto, Nicolas Gif

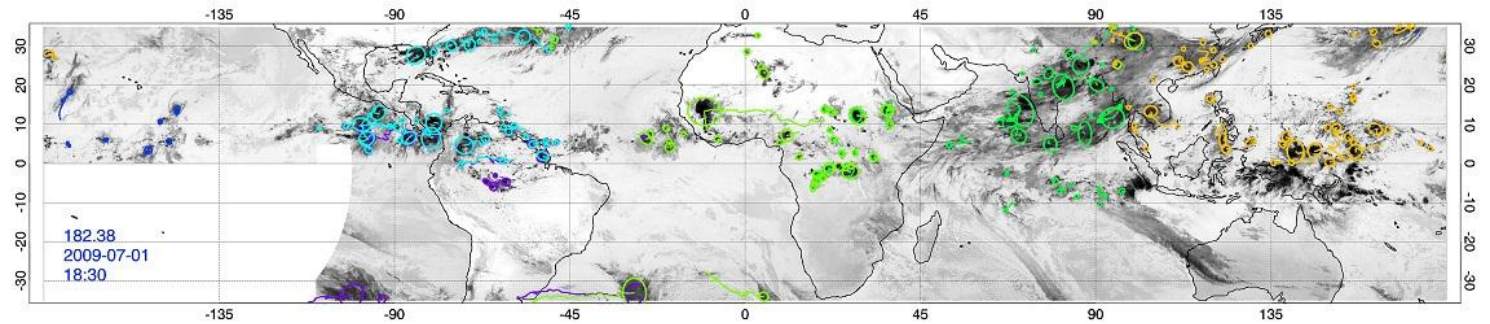

megha-tropiques

March 2012

05

Composite of Convective Systems : a Megha-Tropiques product

Algorithm Theoretical Basis Document

Thomas Fiolleau, Rémy Roca, Jérémie Aublanc, Olivier Chomette, Patrick Raberanto, Nicolas Gif

Laboratoire de Météorologie Dynamique (LMD/IPSL)

March 2012

1 Introduction

Deep convective cloud systems play a major role in the tropical climate by connecting the lower atmosphere to the free troposphere, through the vertical transport of mass, water and momentum. The resulting vertical distribution of associated cumulus-induced heating, cloud radiative cooling and momentum strongly influences the energy and water cycle and the large scale circulation. The vertical profile of net heating and of momentum due to these mesoscale convective systems are driven by the relative contribution of the convective and stratiform processes to the whole cloud system (Houze, 2004). The convective/stratiform fraction within a cloud system hence determines to a large extent its effect onto its environment. It further provides the physical link between the internal system dynamics of MCS (Mesoscale Convective Systems) and large scale environment. The stratiform region is composed of cloud material originating from previously active deep convective cells and therefore confers an utmost importance to the understanding of the time evolution of the broad precipitating characteristics of the mesoscale convective system along its life cycle and the convective/stratiform fraction in particular.

While the geostationary IR (infrared) observations are an invaluable source of information to describe the morphology of the cold cloud shield of the MCS along it life cycle, it falls short as far as the quantitative investigation of the precipitation and microphysical processes and the internal dynamics of the storms are concerned (e.g Liu et al., 2008). One way to overcome the limits of the geostationary IR observations is to combine these morphological parameters with existing exogenous and geophysically relevant products. At the structural level, in a static framework, a number of studies have investigated the scale dependence of the IR derived clusters using various ground-based observations (see Houze and Betts, 1981; Yuter and Houze, 1995) feeding our understanding of the processes underlying the anvil formation and maintenance (Houze, 2004). More recently efforts have been geared towards taking benefit of the active captors on board NASA satellite to investigate the rain and microphysical structural properties of the MCS anvils clusters (e;g., Nessbit et al., 2006).

At the life cycle level, in a dynamic framework, fewer multi observational studies have been performed. Radar measurements obtained during observational campaigns have helped a lot to understand the life cycle of the cold cloud shield of the MCS (Houze, 1982; Williams and Houze, 1987; Diongue et al., 2001; Machado and Laurent, 2004). Beyond individual campaigns, such data fusion approaches, have been successfully implemented taking benefit of surface rainfall observations networks. Based on compositing techniques, such investigation revealed, for instance, key features of the precipitation life cycle of the Mesoscale Convective Complexes over the central

United States (e.g., McAnelly and Cotton, 1989). More recently, these compositing efforts have been extended to the fusion of observations from low earth orbiting satellites together with the life cycle morphology of the MCS derived from geostationary data, mainly over large and oceanic domain, overcoming the limitations induced by the use of regional ground based observing system (Kondo et al 2006, Inoue et al 2009). Futyan and Del Genio (2007) processed METEOSAT Second Generation GERB measurements using the Detect and Spread technique (Boer and Ramanathan, 1997) and an overlap tracking approach to elaborate composite life cycles of MCS over Africa and the Atlantic Ocean region. They further made use of the TRMM radar observations to investigate the internal dynamics of the MCS during the time evolution of its life cycle thanks to a dedicated compositing technique. Their results suggest drastic differences in the life cycle MCS between the Atlantic Ocean and the West African region. Unlike the latter, the MCS over Atlantic Ocean shows steady convective rain fraction along their life cycle. These recent studies have enhanced our conceptual models of the life cycle of organized convection over various regions of the tropics (e.g., Liu et al., 2008 figure 12). These conceptual models are useful to compare to the simulation of Cloud Resolving Models (Futyan and del Genio, 2007; Del Genio, 2011) as well as for the guiding the development of new parameterisation of convection for climate models (Grandpeix and Lafore, 2010; Pritchard et al., 2011; Del Genio, 2011).

To characterize the evolution of the energy budget along the life cycle of convective systems, a Megha-Tropiques level 4 product, called "MCS composite", has been developed using the geostationary IR data as well as the geophysical information derived from the passive remote sensing radiometers MADRAS and ScaRaB (MT level-2 products). This technique merges the MCS morphological parameters derived from the geostationary IR imagery together with the observations from low earth orbiting platforms along the life cycle of the tropical storms. The product and its results will form the core of the operational algorithm (Day-1) for the Megha-Tropiques mission (Roca et al., 2012) and is intended to be applied systematically over the whole intertropical belt during the multi year life of the mission. In this document, the theoretical bases, as well as the technical description of this algorithm are presented. The geophysical products are exemplified for the summer 2009 period over the entire tropical belt, using the TRMM TMI observations, ScaRaB synthetic orbits and the IR data from the fleet of geostationary satellites operating at that time.

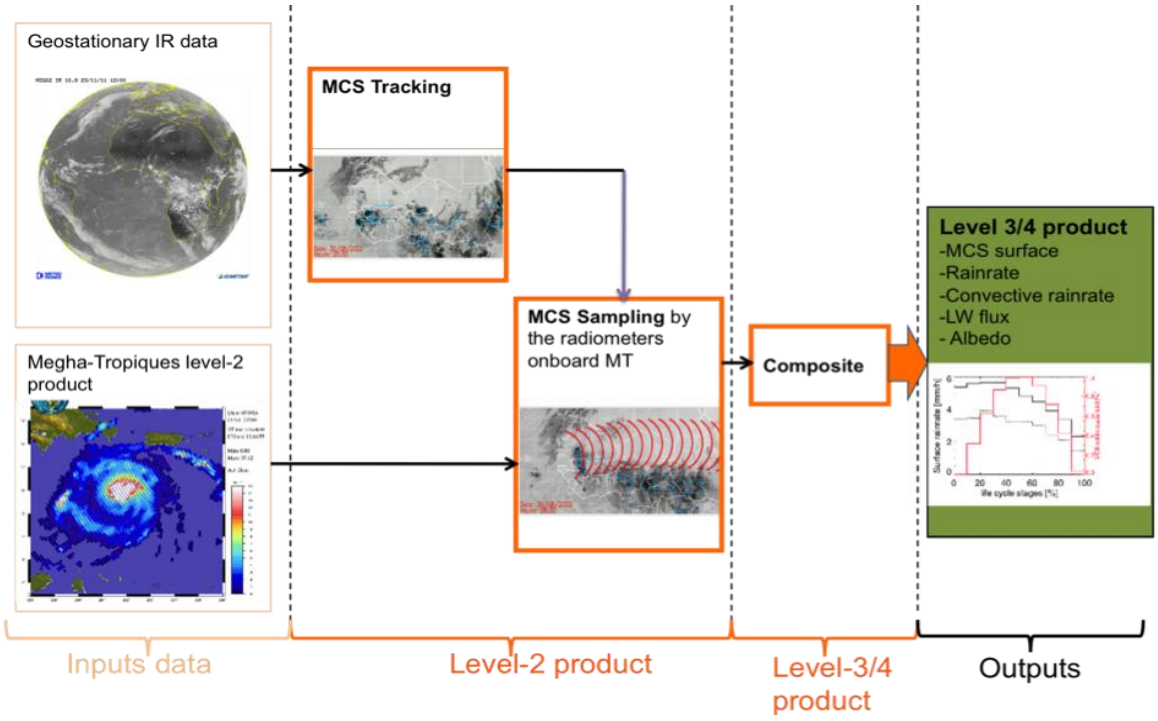

Figure 1: Schematic diagram of the MT product processing.

A schematic of the "MCS composite" level 4 Megha-Tropiques product is presented figure 1 and detailed in the flowchart figure 2. MCS are first detected and tracked from IR geostationary observations allowing the characterization of their morphological parameters along their life cycle. Geophysical characteristics associated to the MCS are determined thanks to a sampling methodology, which merges the IR data from geostationary satellites and Megha-Tropiques observations. An MCS selection and classification is then applied on MCS identified by the tracking algorithm. Finally, composites of MCS are built in order to describe the average evolution of geophysical parameters as well as the cold cloud shield associated to MCS along their life cycle.

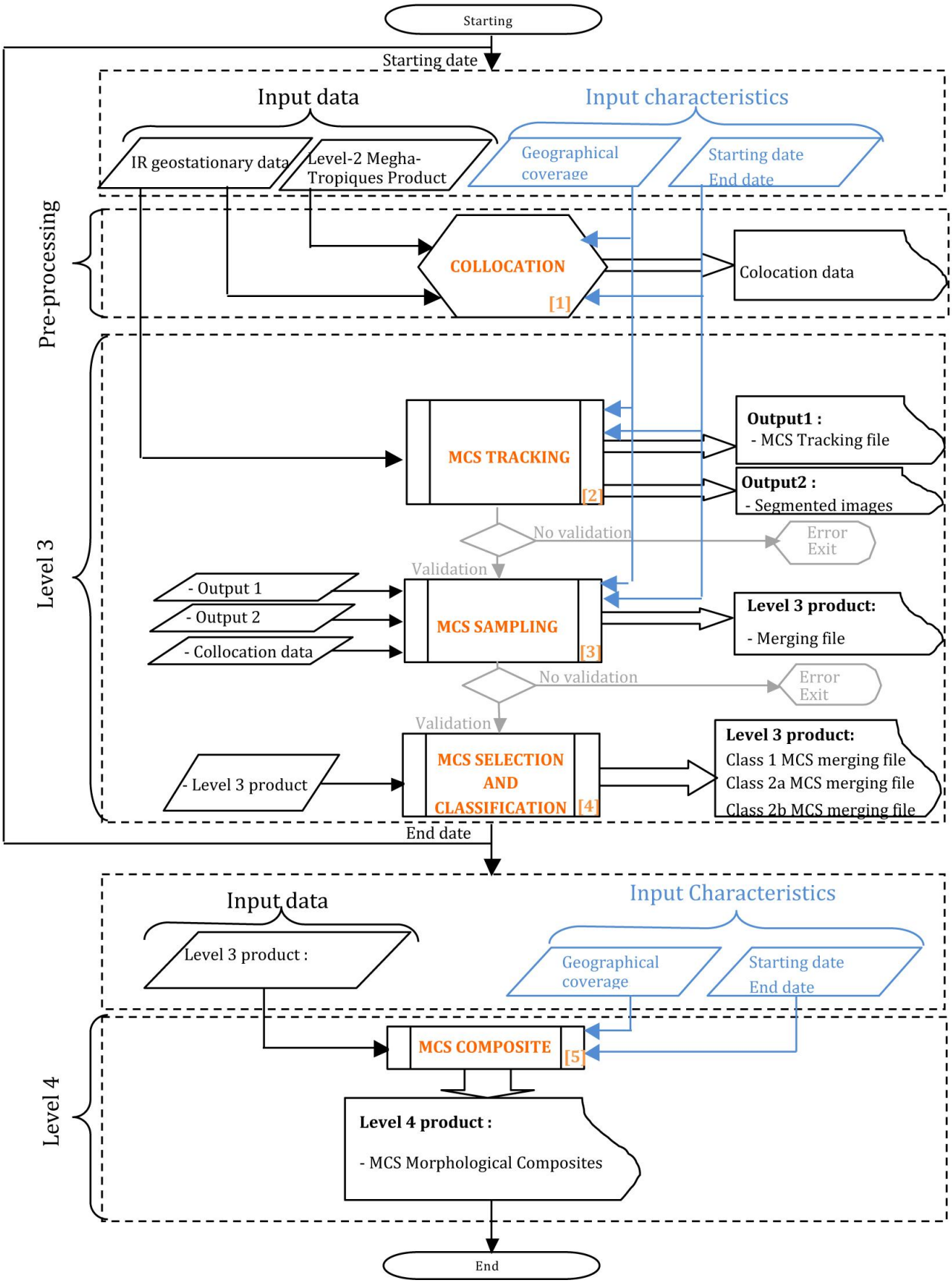

Figure 2: "MCS composite" flowchart

2 Data

2.1 Geostationary Infrared observations

The monitoring of the whole inter-tropical belt is achieved thanks to the use of six geostationary satellites of the operational fleet: MTSAT-1, GOES-10/11/12, METEOSAT-9, and METEOSAT-7 (Figure 3). Depending upon the satellite under considerations, spatial resolution at nadir varies from 3 km for METEOSAT-9 to 5 km for METEOSAT-7. Full disk data from the geostationary satellites are available from at least 15 minutes (METEOSAT-9) to 3 hours (GOES-11/12). The detection and tracking of MCS requires a 30 minutes or better frequency for the infrared images. Such a requirement imposes to make use of subsets of images scanned by the GOES-10/11/12 and MTSAT-1 platforms. Thus, the South American region is scanned by GOES-10 every 15 minutes, while the North American region, the North Pacific region and the Chinese region are monitored by GOES-12, GOES-11 and MTSAT-1 respectively with a 30 minutes frequency.

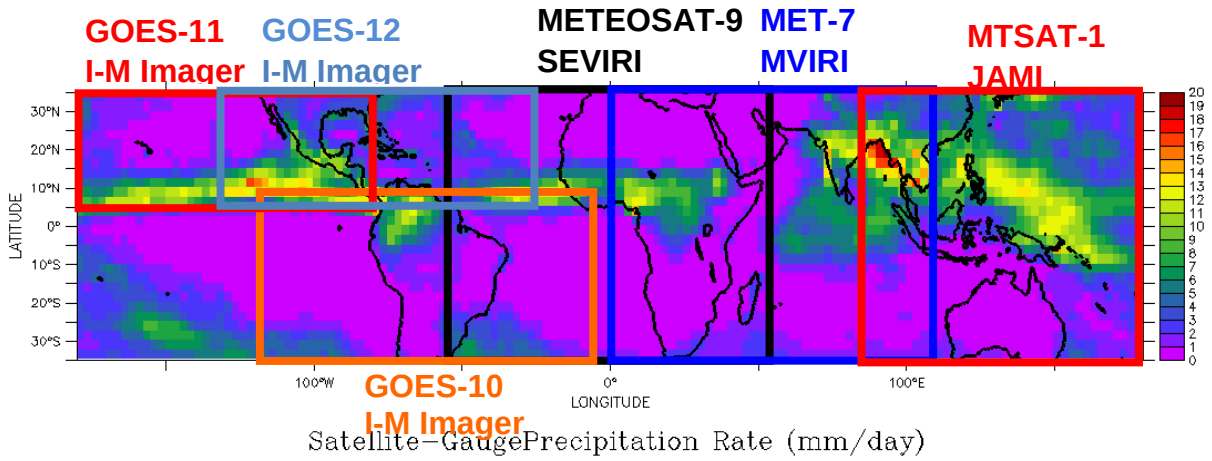

Figure 3 : Spatial Coverage of the Operational geostationary satellites fleet and the associated imagers used to process the entire inter-tropical belt

A quality control step (Szantai et al., 2011) has been applied on time series on each geostationary data, and the percentage of missing images has been computed for the JJAS period in 2009 and reported in Table 1. Table 1 presents also the technical characteristics of the operational geostationary satellites fleet and the associated imagers used for the 2009 monsoonal season. It is to be noticed that the geostationary satellites used could be changed according to their replacement by the satellite agencies.

satellite	Satellite position	Fulldisk Coverage	IR Channels Imagers	Spatial resolution	Time resolution	Tracking Coverage	Lack of data
Goes-10	60°W	None	10.7 µm I-M Imager	4 km	30 min	108°W - 36°W ; 40°S – 0°N	12%
Goes-11	135°W	3h	10.7 µm I-M Imager	4 km	30 min	180°W - 108°W; 0°N – 40°N	1.4%
Goes-12	75°W	3h	10.7 µm I-M Imager	4 km	30 min	108°W - 36°W; 0°N – 40°N	4.8%
METEOSAT-9	0°	15 min	10.8 µm SEVIRI	3 km	15 min	36°W - 36°E ; 40°S – 40°N	0.5%
METEOSAT-7	57.5°E	30 min	11.5 µm MVIRI	5 km	30 min	36°E - 108°E; 40°S – 40°N	5.3%
MTSAT-1	140°E	1h	10.8 µm JAMI	4 km	30 min	108°E - 180°E; 0°N – 40°N	2%

Table 1 : Technical characteristics of the operational geostationary satellites fleet and the associated imagers used to process the entire inter-tropical belt for the monsoonal period in 2009.

2.2 MADRAS observations

The BRAIN retrieval algorithm (Viltard et al. 2006) was originally derived from the GPROF algorithms (Kummerow et al. 2000). The technique is based on a Bayes/Monte-Carlo scheme to retrieve a suite of rainfall information from a vector of measured multi spectral microwave brightness temperatures obtained from a microwave imager. The most probable rain rate is computed from the weighted average of the possible rain rates stored in the retrieval database. The specifics of BRAIN lies in its retrieval database, which is exclusively, made of co-located TMI and PR data. The advantages are namely the absence of errors due to radiative transfer simulation and a natural PDF of the rain events (as seen by the PR). It is important to note that BRAIN does not use any a-priori information during the retrieval process, relying exclusively on the natural PDF of the measured rain and the error-free brightness temperatures stored in its retrieval database. BRAIN provide the Day-1 instantaneous rain estimates from the MADRAS radiometer for the Megha-Tropiques mission (Viltard et al., 2006). In the present study, we use the BRAIN retrievals of the instantaneous surface rain rate (figure 4), as well as the convective/stratiform rain fraction derived from the TMI imager (Kirstetter et al., 2012) for the summer 2009 period over the whole inter-tropical belt.

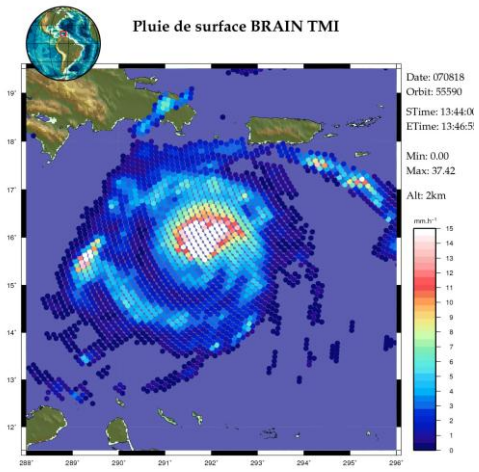

Figure 4 : Illustration of the rainrates estimated by the BRAIN algorithm. (Viltard)

2.3 ScaRaB observations

The Scanner for Radiation Budget (ScaRaB) is a cross-track scanning radiometer with a spatial resolution at nadir of approximately 40 km x 40 km. This instrument has four channels, two broad spectral bands from which the reflected SW and emitted LW radiances at the top of the atmosphere (TOA) are derived, and two narrow bands similar to operational weather satellite imager channels, one corresponding to the infrared atmospheric window, the other to the visible (green to red) portion of the solar spectrum. The calibrated and geolocated radiances from ScaRaB are then converted to hemispherical SW and LW fluxes at the TOA and to the albedo. This conversion is classically obtained by application of scene type and observation geometry-dependent anisotropy models (often referred to as an Angular Dependent Model or ADM). For the ADM issue for ScaRaB in Megha-Tropiques, new neural network techniques have been developed in order to be consistent with the most accurate CERES models (Viollier et al., 2009). The network consists of an input layer (observables), two hidden layers and an output layer (anisotropy factor). This method is independent of explicit scene identification (though networks are generated separately for a small number of surface types and are applicable to all-sky conditions). The created algorithm is called ScaRaB Artificial Neural Network (SANN).

Due to the non-availability of ScaRaB/Megha-Tropiques data, the developments presented in this document were made using data from the GERB instrument on-board MSG (Meteosat Second Generation). We have created ScaRaB/Megha-Tropiques synthetic orbits with the help of IXION software (a satellite orbitography and sampling software, Capderou, 2009, 2012) and with a co-location algorithm (N. Gif et al, 2011), which takes ScaRaB, pixel's point spread function into account.

2.4 Time-space co-location

Geostationary IR observations are used to describe the morphology of the cold cloud shield associated to MCS. However, the analysis of the geophysical features associated to MCS along their life cycle can't be achieved from geostationary satellites alone. To reach this goal, a sampling technique is developed to merge the MCS morphological parameters derived from the geostationary infrared imagery together with the observations from low earth orbiting platforms like MT, along the life cycle of the storms.

Geophysical information from the MADRAS and the ScaRaB level-2 products for precipitating structures and radiation budget respectively are also taking into account.

A space/time colocation between the above MT level 2 products and geostationary data is performed using the following specifications:

- a 15 minutes maximum time interval between two observations is allowed (half the standard time resolution of a 30 minutes geostationary temporal acquisition scheme).
- different spatial co-location methods are used according to the instrument considered. A methodology called 2DI method has been developed for data from ScaRaB instrument that takes pixel's point spread function (PSF) into account (i.e. the real shape of pixels) (Gif et al 2011). For the MADRAS instrument, a nearest-neighbor method has been elaborated, assuming that the MT level 2 MADRAS products cover circular areas of 20 km diameter.

3 The Algorithms

3.1 MCS Tracking

The « MCS Tracking » step corresponds to the detection and the tracking of the MCS from IR geostationary data. The algorithm used is fully detailed in a number of papers (Williams and Houze 1987, Arnaud et al 1992, Mathon and Laurent 2001). The flowchart of this "MCS tracking" step is presented Figure 4 and described table 1. The tracking algorithm is composed of two steps :

1. the detection at a given time
2. the tracking of the tropical convective systems along the time.

The detection step is based on a segmentation of the IR geostationary images by a simple cold brightness temperature threshold to delineate continuous regions in space that is colder than a threshold. The Tb (Brightness Temperature) threshold is set at 233K, well adapted to detect tropical MCS (figure 5).

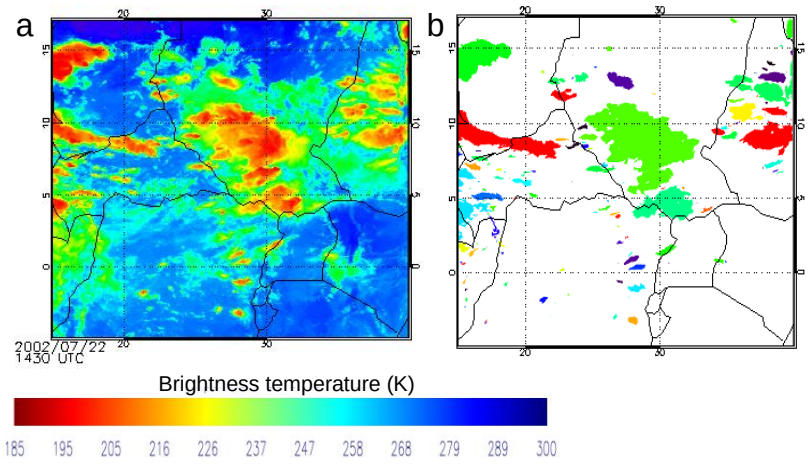

Figure 5 : Illustration of the IR image segmentation by a 233K threshold for a convective situation which occurred on July 22th 2002 over the Ethiopian region. a) IR image from MET-7. b) Result of the IR image segmentation by a 233K threshold. Each color corresponds to a single convective cluster.

The cloud clusters detected in the image at time *t+1* are matched with the ones in the previous image at time *t* based on the spatial overlap between the two segmented images. Convective clusters are matched if the overlap is greater than 50% or 10000km² of the area of either the current cluster or the cluster from the previous image. A cloud system is considered to originate when no overlapping occurs in the previous image. On the other hand, a convective system dissipates when there is no longer intersection with another cluster in the next image. Thus a convective system is defined as a succession of convective clusters, which have been segmented in successive images (figure 6).

The tracking can result in some clusters merging and splitting yielding to complex MCS life cycle. When several clusters merge to form a unique cluster in the next image, the larger cluster at this time is selected to continue the original track, whereas the tracks of the smaller clusters are considered to end. Similarly, split clusters are taking into account by selecting the larger cluster in the next image to continue the track while the smaller cloud clusters are considered as split generation.

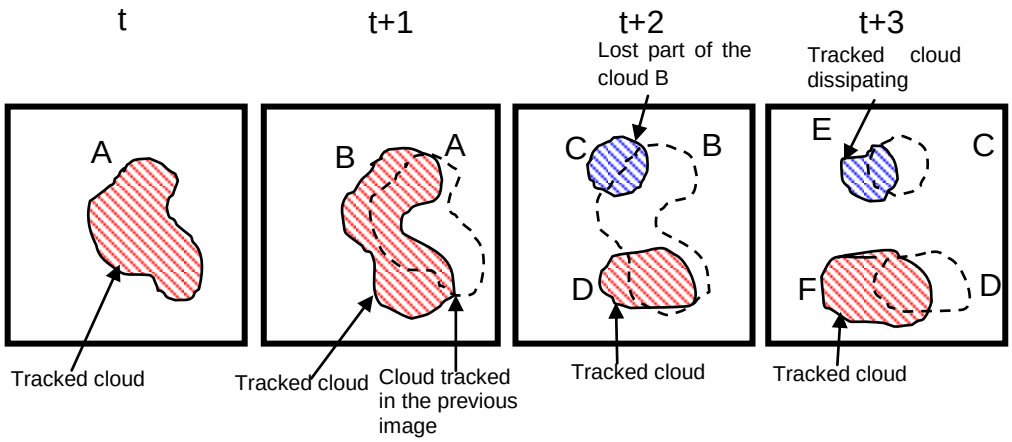

Figure 6 : Illustration of the tracking methodology based on the area-overlapping technique for successive time steps.

Missing images in the time series are handled as follows: if few images are missing, a recovery process is run to continue the track of each convective system during the period of missing images. This process is based on the generation of the missing images, by extrapolating the behavior of each convective system (locations, cold cloud surface). The maximum number of successive missing images has been set to 10 images (5h for a 30-minute geostationary temporal resolution). Using the tracking algorithm MCS morphological parameters are documented, such as the surface of the system (km^2), the mean brightness temperature (K), the propagation speed (m/s) as a function of time along the MCS life cycle (table n). Integrated MCS characteristics are also computed : the lifetime duration (hr), the MCS genesis and lysis date, the cumulated surface, the average speed.

The tracking algorithm is applied to the full tropical band using the geostationary infrared data of six different satellites (GOES10, GOES11, GOES12, METEOSAT-9, METEOSAT-7, and MTSAT). It is to be noticed that each satellite data is processed independently and a MCS tracking file is elaborated for each geostationary satellite (figure 7).

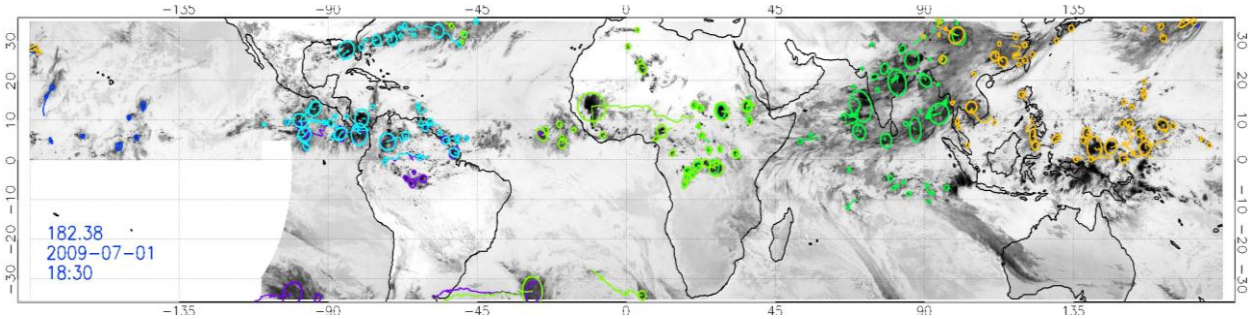

Figure 7: Illustration of the MCS tracking in July 2009. Each color corresponds to the tracking of MCS for a given geostationary satellite.

3.2 MCS Sampling

Objective of the "MCS Sampling" step is to merge the MCS morphological characteristics identified previously by the tracking algorithm with the Megha-Tropiques level-2 products derived from MADRAS and SCARAB in order to compute average geophysical characteristics of MCS within its life cycle. The BRAIN retrieval algorithm (MT level-2 product) is used to merge precipitating data with the morphology of the MCS, while the earth radiation budget information is merged with the MCS characteristics by using the SANN algorithm (MT level-2 product).
The average geophysical characteristics can then be computed for each convective cluster sampled by the MADRAS (SCARAB) instrument. Thus, the "MCS Sampling" step documents geophysical parameters (average conditional rainrate (mm/h), average LW radiation (W/m^2)….) associated to MCS for some steps of their life cycles.

Figure 8 illustrates the sampling of a MCS by the MADRAS instrument over the Indian region. The MCS, lasting 35h, is sampled eight times by the MADRAS instrument within its life cycle. The detected clusters are represented by an ellipse (red when the Cluster is sampled by the MADRAS/MT instrument and grey when the MCS is not sampled). The MT orbit (simulated) is colored in blue, while the MCS trajectory is represented in green.

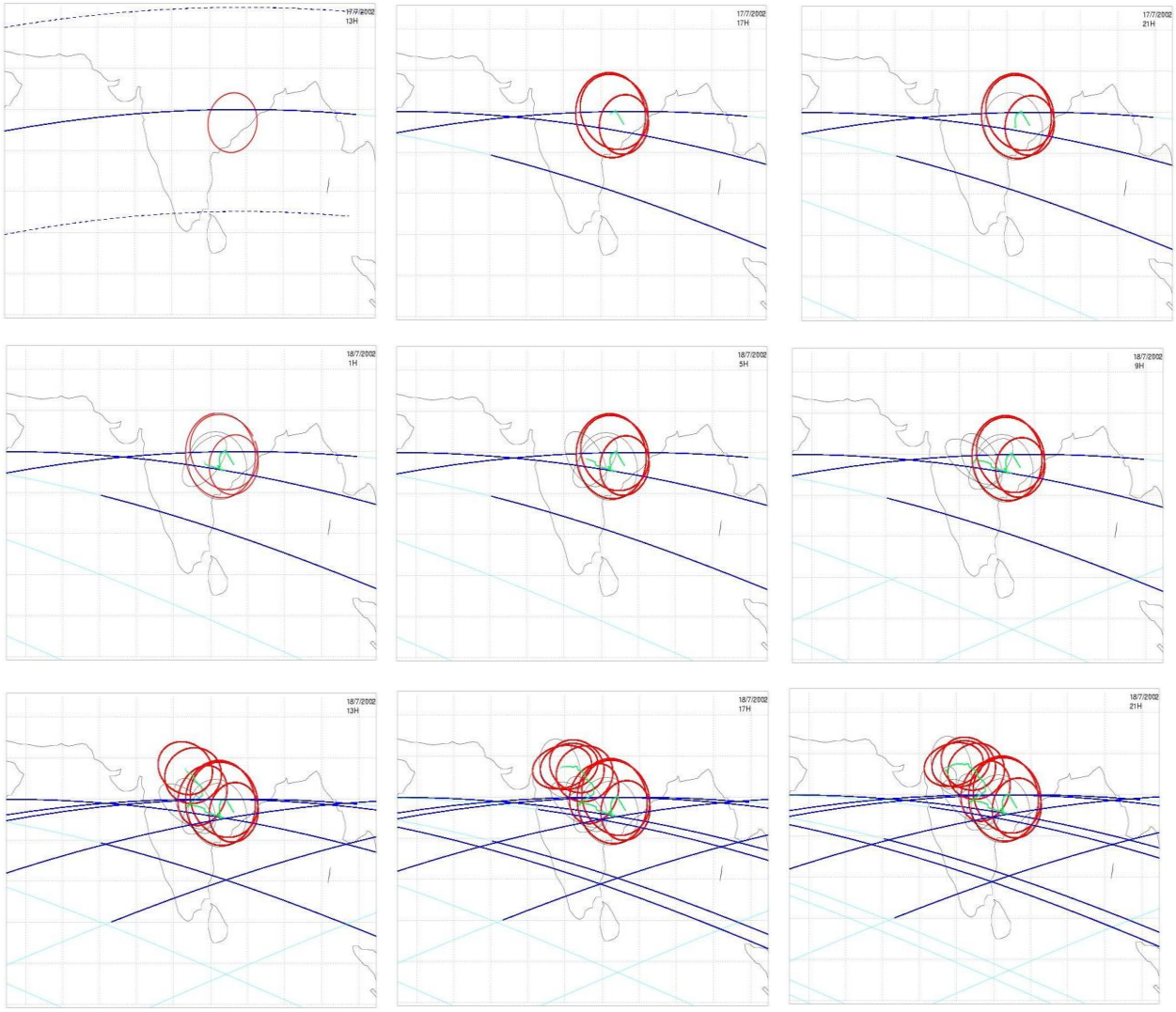

Figure 8: Illustration of an MCS sampling by MADRAS/MT over the Indian continent.

3.3 MCS selection and classification

In order to analyze convective systems describing a complete life cycle, the "MCS selection and Classification" step is applied. This step first filters MCS generated by a split, or dissipated by a merge.

	Definition	
Class 1	Lifetime duration < 5h	
Class 2	Lifetime duration > 5h	a- MCS describing only one maximum
		b- The others (several maximum)

Table 2 : Definition of the MCS classes

MCS are then selected according to their lifetime duration and two classes are computed (table 2):

- MCS lasting less than 5h belonging to the class 1,
- MCS lasting more than 5h belonging to the class 2.

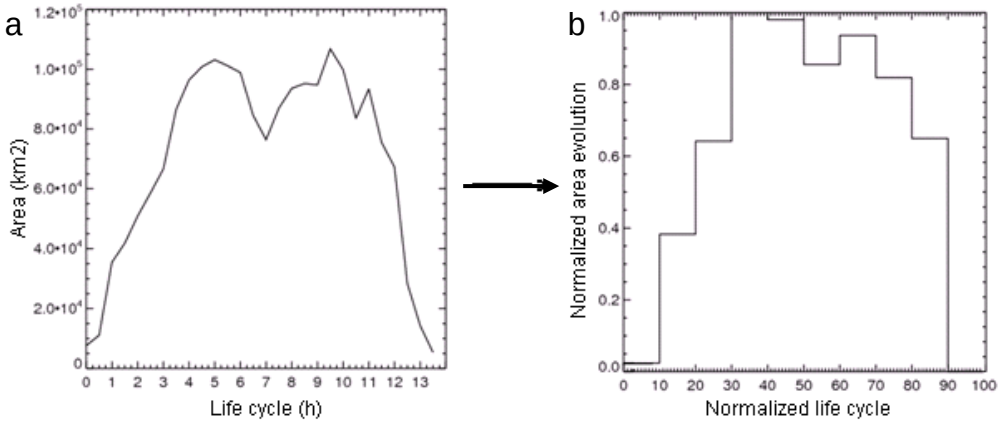

Figure 9: a) MCS surface evolution and b) its life cycle normalization .

The life cycle of the MCS belonging to class 2 are then normalized (figure 9). The lifetime is normalized between 0 and 100% and discretised in ten steps. Similarly, the cold cloud surface is normalized between 0 and 1. Figure 9 illustrates the evolution of the MCS cold cloud surface and the corresponding MCS life cycle normalization.

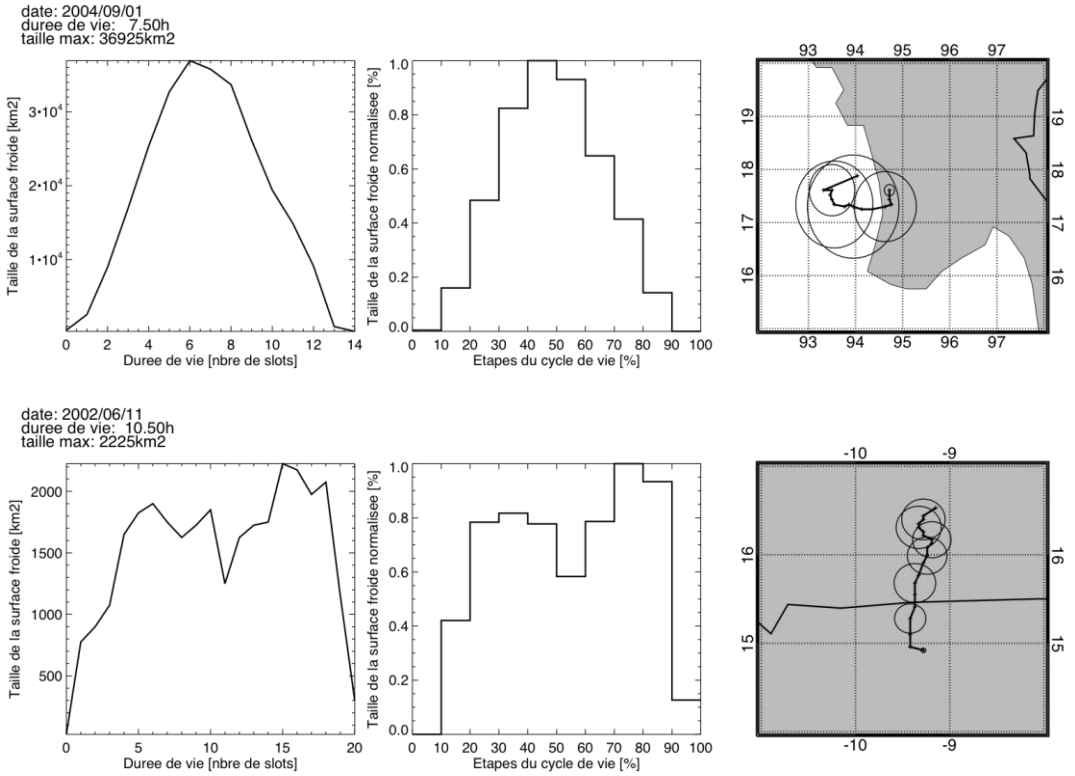

Figure 10: Illustration of a MCS belonging to class 2a; class 2b (below)

MCS are then be classified according to the evolution of their cold cloud shield. MCS which depicts a single maximum in surface area during its life cycle are attributed to class 2a while the rest (MCS having several surface area maximums) are attributed to class 2b.

4 The MT level-4 product: "MCS composite"

4.1 Methodology

The level-4 "MCS composite" algorithm generates composites of geophysical parameters associated to the MCS belonging to the class 2a for a given period and a defined geographical domain. The algorithm uses MCS belonging to the class 2a as input as well as domain and time specifications (geographical domain, time period).

MCS sampled by the MADRAS and SCARAB radiometers are then selected according to the specified geographical area and time period. With respect to the spatial sampling, the limited swath of the MT instruments have to be accounted for, as only a portion of individual convective clusters may be sensed by a radiometer, by lowering its significance at the system scale. Larger the cluster, lower the probability that the cluster surface area is totally matched. Similarly, small swath width of the microwave instrument adds difficulties to match the entire surface of convective cluster. A quality index limit set at 70% is then applied on the fraction of the cluster covered with the radiometer instruments.

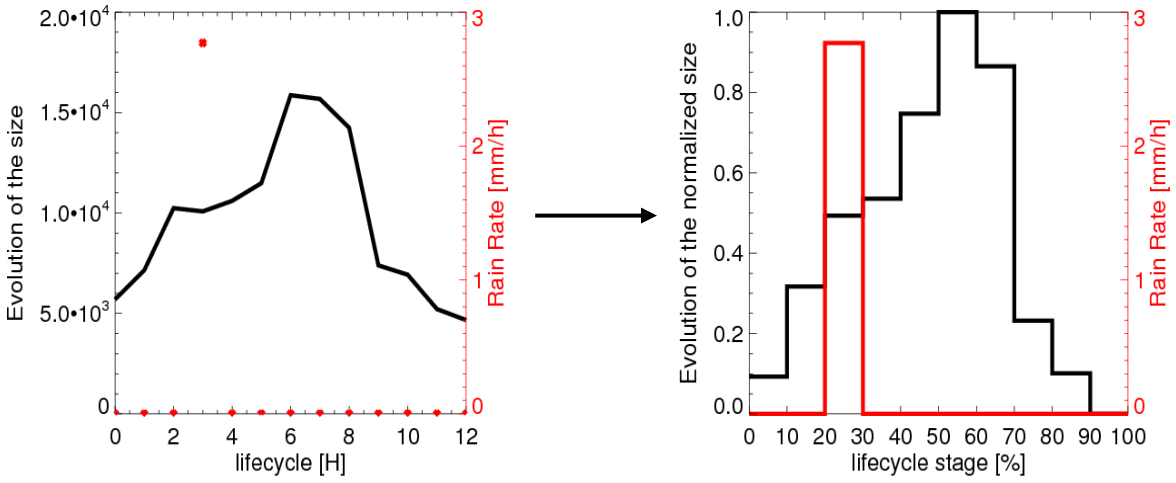

Figure 11: Normalization of the MCS life cycle in ten steps. The rainrate measured in the third hour of the MCS life cyle is projected within the [20%-30%] step of the normalized life cycle.

The life cycles of the selected MCS are then normalized and discretised in ten steps between 0% and 100%. The geophysical characteristics measured within a MCS life cycle are then projected into the corresponding step of the MCS normalized life cycle (figure 11).

A continuous view of each geophysical parameter is then computed along the life cycle of the MCS composite. Figure 12 illustrates the compositing methodology for the rainrate parameter.

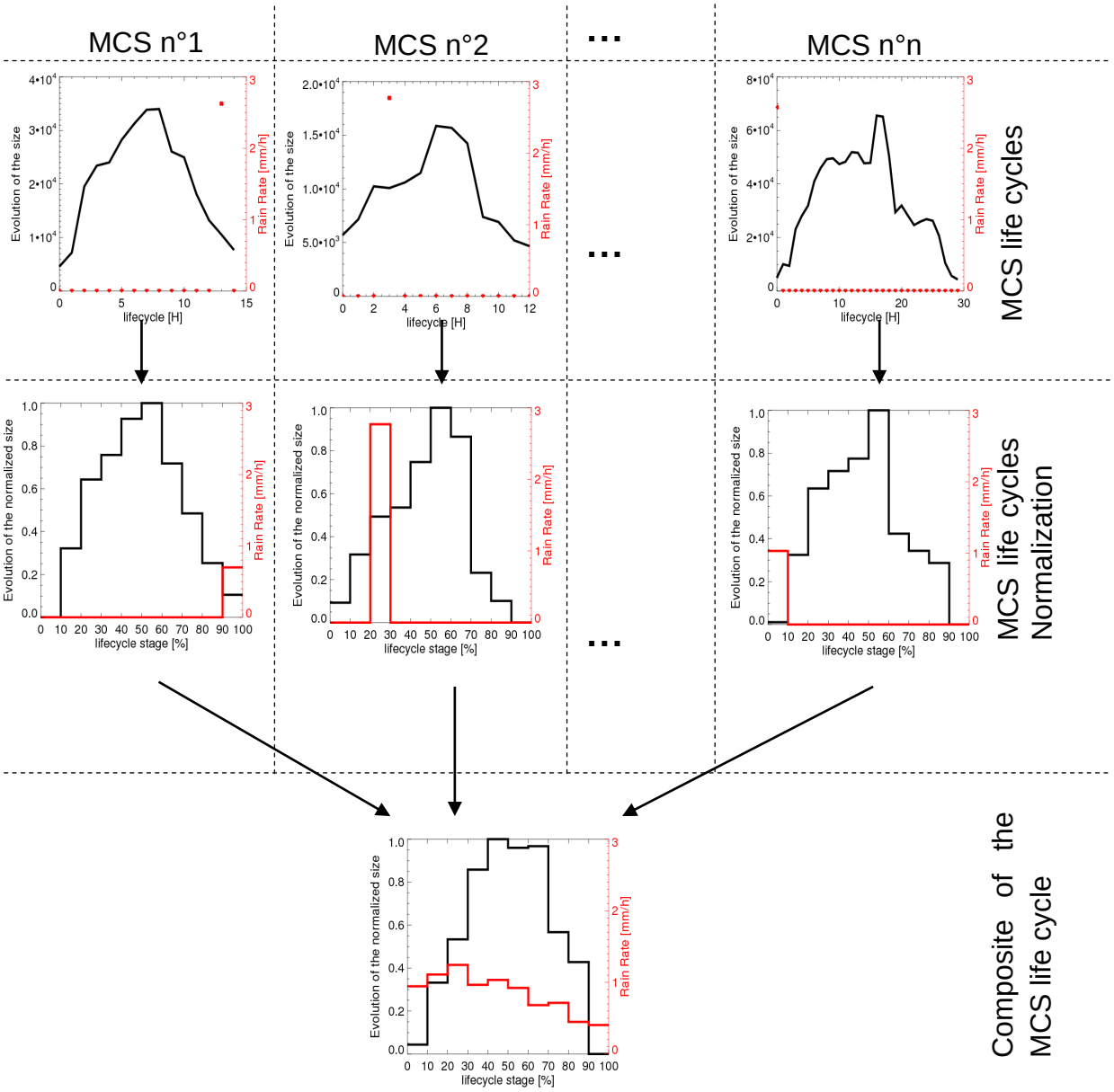

Figure 12: Scheme of the compositing methodology

4.2 Specifications

To underline the MCS behaviours of different tropical regions, several geographical domains are specified. Using the 1998-2011 rainfall climatology derived from the TRMM 3B43 product (figure 13), five regional domains have been specified according to the localisation of precipitation:

- Pacific regional domain : 180°W, 85°W / 20°S, 20°N
- South America regional domain : 85°W, 35°W / 35°S, 15°N
- Atlantic and Central Africa regional domain : 35°W, 40°E / 20°S, 20°N
- Indian Continent and Ocean domain : 40°E, 105°E / 30°S, 35°N
- Indonesia and West Pacific domain : 105°E, 180°E / 20°S, 35°N

For each region, MCS composites are computed separately for continental, oceanic and coastal conditions. Composites are also generated for the entire tropical belt. Moreover, four study periods have been established corresponding to different seasons:

- Winter : January, February, March
- Spring : April, May, June
- Summer : July, August, September
- Autumn : October, November, December

For each region of interest, MCS composites are computed for continental, oceanic and coastal conditions. Composites are also computed for diurnal conditions. Clusters sampled by MADRAS from 6h to 18h (local hour) are selected for the computation of the rain parameters of the diurnal composite. Clusters sampled by SCARAB with a measurement of the albedo are selected for the computation of the earth radiation budget parameters of the diurnal composite

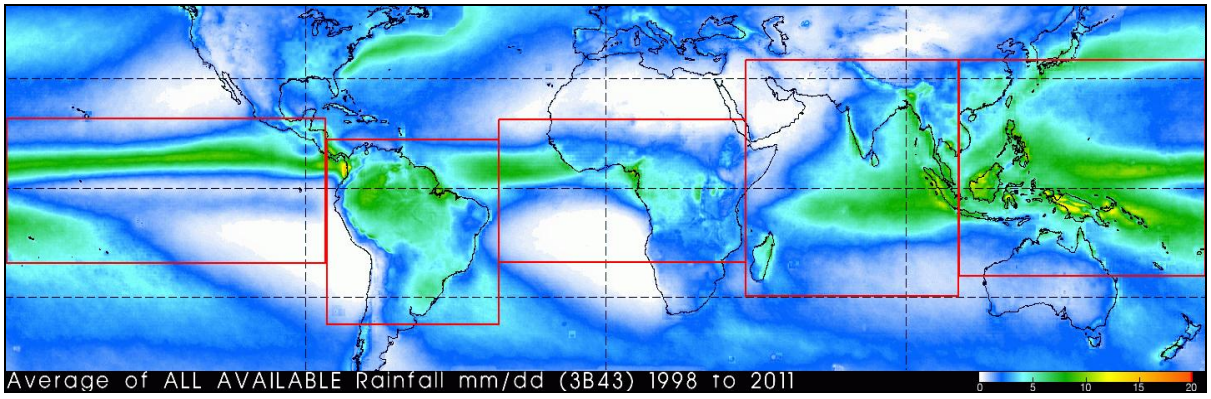

Figure 13: Specification of regional domains for the four period of study according to the 1998-2011 climatology derived from the 3B43 data.

4.3 Illustration of a MCS composite

An illustration of MCS Composites over the African region (40°S-40°N; 60°W-60°E) and derived from the fleet of IR geostationary data, TMI/TRMM observations and SCARAB/MT synthetic orbits are presented figures 14 and 15 for the months of June-September 2009, for both diurnal and nocturnal conditions.

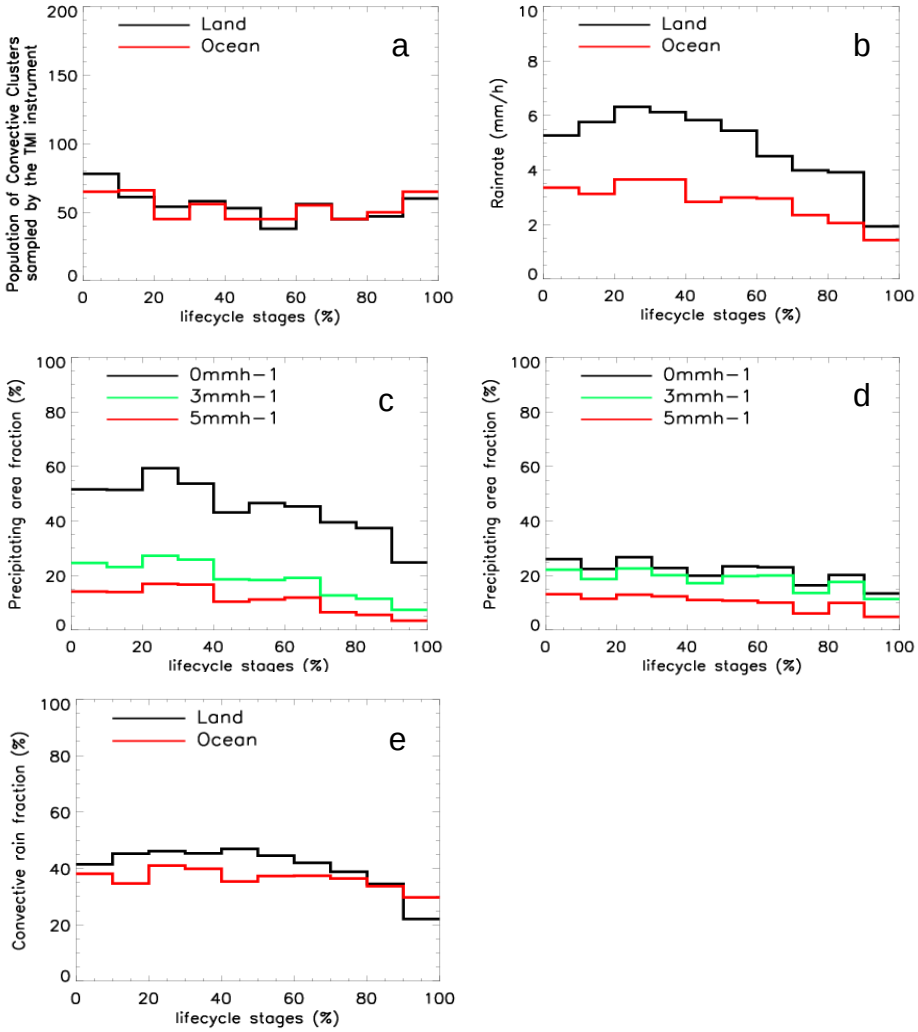

Figure 14: a) Population of the convective clusters sampled by TMI/TRMM. b) Evolution of the conditional average surface rainrate associated to continental (black line) and oceanic (red line) convective systems over the African region for the JJAS period in 2009. c) d) Evolution of the precipitating area fraction for the continental and the oceanic convective systems. e) Evolution of the convective rain fraction for the continental (black) and the oceanic (red) convective systems.

The average evolution of conditional rainrate and precipitating fraction associated to MCS along their life cycle is presented in figure 14b. The black line corresponds to the Continental MCS and the red one represents the Oceanic MCS. In order to better understand the strong difference between the land and oceanic regimes over both monsoon regions, the distribution of the rain rate within the

systems are investigated in figures 14c and figure 14d. The evolution of the convective rain fraction associated to MCS along their life cycle is shown in figure 14e. Figure 14a shows the population of convective clusters sampled by the TMI/TRMM instrument for each step of the normalized life cycle. Fiolleau and Roca (2012) discuss in detail the evolution of the precipitating features for the JJAS 2009 period over the entire tropical belt.

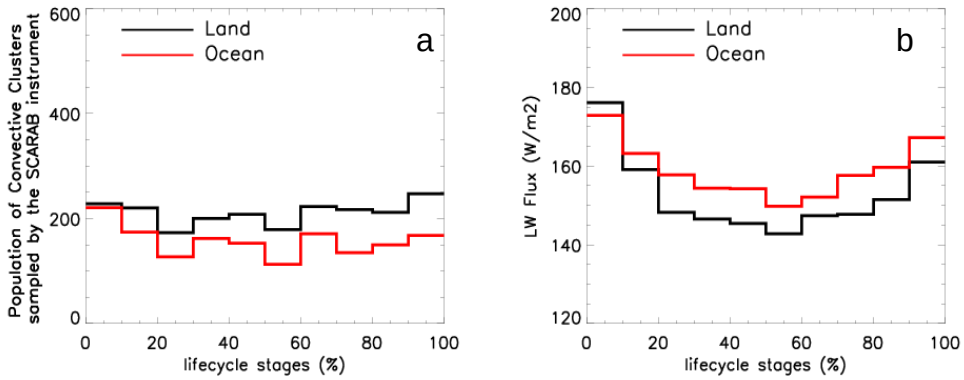

Figure 15: a) Population of the convective clusters sampled by SCARAB/MT. b) Evolution of the LW flux (W/m^2) associated to continental (black line) and oceanic (red line) convective systems over the African region for the JJAS period in 2009.

Figure 15b shows the evolution of the LW (Long Wave) flux associated to the MCS along their life cycle for daily and night conditions over the African region and for the JJAS period. The population of clusters for each step of the life cycle is shown in figure 15a. We can observe for both continental and oceanic regions a decrease of the LW flux up to the 20%-30% step of the normalized life cycle from 175 w/m2 to 150 w/m2 for continental systems and 140 w/m2 for oceanic systems. Then, the LW flux seems to be stable at 150 w/m2 (140 w/m2) for continental (oceanic) conditions between the 30% and the 80% steps, and increases up to the end of the MCS life cycle to reach 165 w/m2 (160 w/m2).

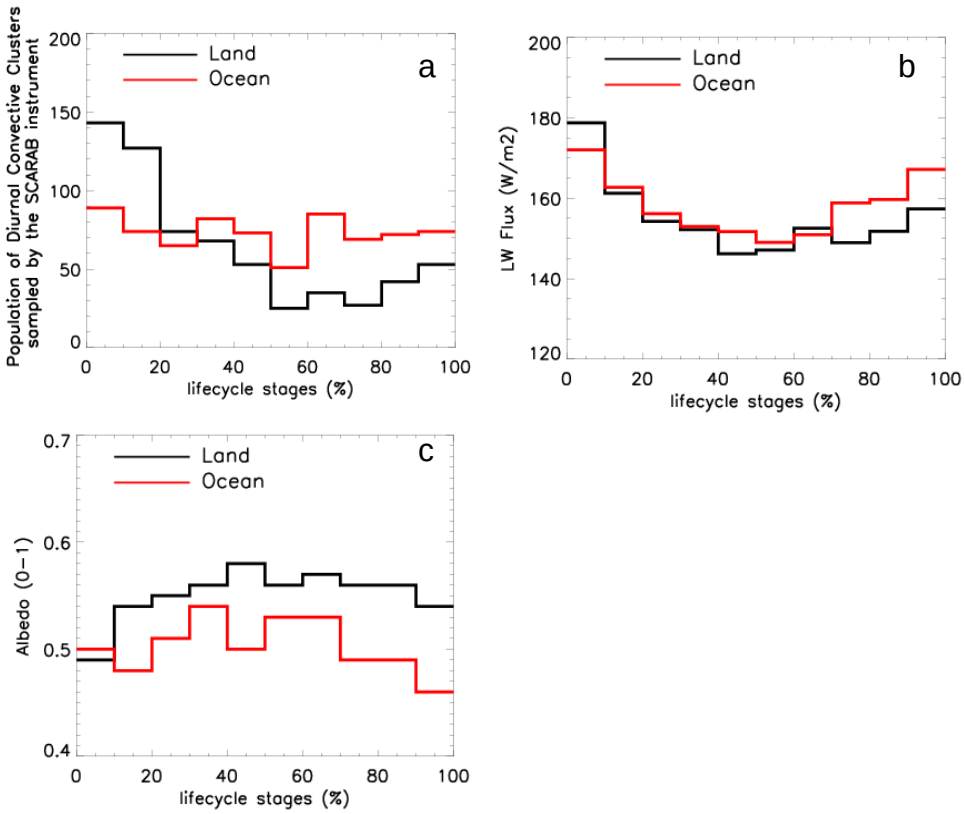

Figure 16: a) Population of the convective clusters sampled by SCARAB/MT for diurnal conditions. b) Evolution of the LW flux (W/m^2) associated to continental (black line) and oceanic (red line) convective systems over the African region for the JJAS period in 2009. c) Evolution of the albedo (0-1) associated to continental (black line) and oceanic (red line) convective systems over the entire tropical belt for daily conditions.

The diurnal evolution of LW flux and albedo parameters associated to MCS is presented in figure 16b and 16c for diurnal conditions for the inter-tropical belt region and for the JJAS 2009 period. These first results show that the evolution of the LW radiation seems to be similar for diurnal and nocturnal conditions. An increase in albedo can be observed from 0,49 to 0,58 up to 50% of the continental MCS life cycle followed by a low decrease at the end of the MSC life cycle.

REFERENCES

Arnaud, Y., M. Desbois, J. Maizi (1982). Automatic Tacking and Characterization of African Convective Systems on Meteosat Pictures**,** Journal of Applied Meteorology, 31(5), PP.443-453.

Boer, E. and V. Ramanathan (1997). Lagrangian Approach for Deriving Cloud Characteristics from Satellite Observations and its Implications to Cloud Parameterization. J. Geophys. Res., **102** (D17), pp. 21 383–21 399.

Capderou, M. (2009). Sampling. Megha-Tropiques Technical Memorandum n°1

Capderou, M. (2012). Satellites: de Kepler au GPS, 866 p., Ed. Springer, Berlin, Paris.

Del Genio, A.D (2011). Representing the sensitivity of convective cloud systems to tropospheric humidity in general circulation models. Surv. Geophys., doi:10.1007/s10712-011-9148-9.

Diongue, A. (2001). Interactions entre convection et écoulement de grande échelle au sein de la mousson de l'Afrique de l'Ouest. Thèse de doctorat, Université Paul Sabatier de Toulouse, Toulouse.

Fiolleau, T., and R. Roca (2012). Composite life cycle of tropical mesoscale convective systems from geostationary and low earth orbit satellites observations: method and sampling considerations. Submitted to Q. J. R. Meteorol. Soc.

Futyan, J. M. and A. D. Del Genio (2007). Deep Convective System Evolution over Africa and the Tropical Atlantic. Journal of Climate, **20** (20), pp. 5041–5060.

Gif, N., O. Chomette, P. Raberanto (2011). Co-location algorithm: Geophysical data projection using pixel point spread function. Megha-Tropiques Technical Memorandum n°2

Grandpeix, J-Y and JP. Lafore (2010). A density current parametrization coupled to Emanuel's convection scheme. Part I: the models. Journal of the Atmospheric Sciences, **67**: 881 – 897. DOI: 10.1175/2009JAS3044.1.

Houze, R. A. (1982). Cloud Clusters and Large-Scale Vertical Motions in the Tropics. J. Meteorol. Soc. Japan, **60** (1), pp. 396–408.

Houze, R. A. (2004). Mesoscale convective systems. Rev. Geophys., **42** (4), pp. 8755–1209.

Houze, R. A., Jr., and A. K. Betts (1981), Convection in GATE, Rev. Geophys., *19*(4), 541–576, doi:10.1029/RG019i004p00541.

Inoue, T., D. Vila, K. Rajendran, A. Hamada, X. Wu and L. A. T. Machado (2009). Life Cycle of Deep Convective Systems over the Eastern Tropical Pacific Observed by TRMM and GOES-W. Journal of the Meteorological Society of Japan, **87A**, pp. 381–391.

Kirstetter, P.E., N. Viltard and M. Gosset (2012). An error model for instantaneous satellite rainfall estimates: evaluation of BRAIN-TMI over West-Africa. Q. J. R. Meteorol. Soc., in press.

Kondo, Y., A. Higuchi, K. Nakamura (2006). Small-Scale Cloud Activity over the Maritime Continent and the Western Pacific as Revealed by Satellite Data. Monthly Weather Review, **134** (6), pp. 1581–1599

Kummerow, C., J. Simpson, O. Thiele, W. Barnes, A. T. C. Chang, E. Stocker, R. F. Adler, A. Hou, R. Kakar, F. Wentz, P. Ashcroft, T. Kozu, Y. Hong, K. Okamoto, T. Iguchi, H. Kuroiwa, E. Im, Z. Haddad, G. Huffman, B. Ferrier, W. S. Olson, E. Zipser, E. A. Smith, T. T. Wilheit, G. North, T. Krishnamurti et K. Nakamura (2000). The Status of the Tropical Rainfall Measuring Mission (TRMM) after Two Years in Orbit. J. Appl. Meteorol., **39** (12), pp. 1965–1982.

Liu,C., E.J. Zipser, D.J. Cecil ,S.W. Nesbittet, S. Sherwood (2008).A Cloud and Precipitation Feature Database from Nine Years of TRMM Observations. Journal of Applied Meteorology and Climatology, **47** (10), pp. 2712–2728.

Machado, L. A. T. and H. Laurent (2004). The Convective System Area Expansion over Amazonia and Its Relationships with Convective System Life Duration and High-Level Wind Divergence. Monthly Weather Review, **132** (3), pp. 714–725.

McAnelly, R.L. and W.R. Cotton(1989).The Precipitation Life Cycle of Mesoscale Convective Complexes over the Central United States. Monthly Weather Review, **117** (4), pp. 784–808.

Mathon, V. and H. Laurent (2001). Life cycle of Sahelian mesoscale convective cloud systems. Quart. J. Roy. Meteorol. Soc., 127, pp.377-406.

Nesbitt, S. W., R. Cifelli and S. A. Rutledge (2006). Storm Morphology and Rainfall Characteristics of TRMM Precipitation Features. Monthly Weather Review, **134** (10), pp. 2702–2721.

Pritchard, M. S., M. W. Moncrieff and R. C. J. Somerville (2011). Orogenic propagating precipitation systems over the US in a global climate model with embedded explicit convection. In Press, Journal of the Atmospheric Sciences

Roca R, et al. (2012). The Megha-Tropiques mission: presentation and scientific objectives. In preparation for Q. J. R. Meteorol. Soc. Special Issue on Megha-Tropiques.

Szantai, A., B. Six, S. Cloché, G. Sèze (2011). Quality of geostationary satellite images. Megha-Tropiques Technical Memorandum n°3

Viltard, N., C. Burlaud and C. D. Kummerow (2006). Rain Retrieval from TMI Brightness Temperature Measurements Using a TRMM PR-Based Database. Journal of Applied Meteorology and Climatology, **45** (3), pp. 455–466.

Viollier, M., C. Standfuss, O. Chomette and A.Quesney (2009). Top-of-Atmosphere Radiance-to-Flux conversion in the SW domain for the ScaRaB-3 instrument on Megha-Tropiques. J. Atmos. Oceanic Technol., 26, 2161-2171.

Williams, M. and R. A. Houze (1987). Satellite-Observed Characteristics of Winter Monsoon Cloud Clusters. Monthly Weather Review, **115** (2), pp. 505–519.

Yuter, S. E. and R. A. Houze (1995). Three-Dimensional Kinematic and Microphysical Evolution of Florida Cumulonimbus. Part I : Spatial Distribution of Updrafts, Downdrafts, and Precipitation. Monthly Weather Review, **123** (7), pp. 1921–1940.

MTTM

Megha-Tropiques Technical Memorandum

Laboratoire de Météorologie Dynamique (LMD / IPSL)

Ecole Polytechnique

F-91128 Palaiseau

France

Sophie.Bouffies-Cloche@ipsl.jussieu.fr

http://meghatropiques.ipsl.polytechnique.fr/available-documents/mttm/index.html